Spiral wave dynamics in oscillatory inhomogeneous media

Matthew Hendrey, Edward Ott, and Thomas M. Antonsen, Jr.
Department of Physics and Institute for Plasma Research, University of Maryland, College Park, Maryland 20742
(Received 12 May 1999; revised manuscript received 3 January 2000)

The effect of a long length scale static inhomogeneity on spiral wave dynamics is studied in the two-dimensional complex Ginzburg-Landau equation. We find that the inhomogeneity leads to the formation of a dominant spiral domain that suppresses other spiral domains, and that the spiral vortices slowly drift in the presence of an inhomogeneity with a velocity that is proportional to the local parameter gradients. We derive an expression for the spiral vortex drift velocity and present examples of both fixed point and limit cycle attractors of the spiral vortices.

PACS number(s): 82.40.Ck, 47.32.Cc, 47.54.+r

I. INTRODUCTION

In many situations it has been observed that spiral wave patterns play a dominant role in system dynamics. Examples of spiral waves can be found in areas of biology, chemistry, and physics. Spiral waves of the electrical signal in the heart occur in cardiac arrythmias [1,2]. Chemical reaction-diffusion systems, such as the Belousov-Zhabotinsky reaction, exhibit spiral waves [3]. Spiral waves also appear in slime mold colonies of *Dictyostelium* [4,5] and planar dc driven semiconductor-gas discharge systems [6]. Our work investigates the effects of a spatial inhomogeneity of the supporting medium on spiral waves. Most physical systems can have an inhomogeneity. For example, spiral waves in cardiac arrythmias encounter inhomogeneities inherent in the cardiac tissue due to cell variations. An inhomogeneity in a chemical reaction-diffusion system can arise from a temperature gradient or inhomogeneity of the gel or porous medium in which the experiments are often performed. References [7,8] studied the light-sensitive Belousov-Zhabotinsky reaction and varied the chemical reaction rate using its sensitivity to light intensity. We suggest that some of the results of our paper might be conveniently tested by arranging the light intensity to vary spatially across the entire system. Another test of our results could use the method described in [9], which uses an inkjet printer to apply a chemical catalyst in the Belousov-Zhabotinsky reaction, to create a spatially varying catalyst. In *Dictyostelium* experiments, Ref. [5] reports an excitation inhomogeneity due to the sorting of prestalk and prespore cells.

In the past much work has been done to investigate inhomogeneities in spiral wave systems covering analytical, experimental, and numerical studies. Analytic work has looked at the effects of parameter gradients on spirals, including drift of spiral centers (vortices) [10,11]. Inhomogeneities have also been studied in biological [5,12] and chemical [7,9,13,14] experiments. Numerical studies of inhomogeneities cover drift of spiral centers due to parameter gradients [15–17] and localized inhomogeneities [18–20].

In this paper we report on spiral waves in oscillatory media under the influence of a time independent, slowly varying spatial inhomogeneity. After spirals first form, the inhomogeneity causes spirals that are favorably located to widen their domains at the expense of less favorably located spirals. The spiral vortices also slowly drift due to the inhomogeneity and results for the velocity of the spiral vortices are given in terms of the gradients of the inhomogeneity.

A very general model exhibiting spiral wave solutions is the two-dimensional complex Ginzburg-Landau equation (CGLE),

$$\partial_t A = \mu A - (1+i\alpha)|A|^2 A + (1+i\beta)\nabla^2 A, \tag{1}$$

where $A(x,y,t)$ is complex. This equation describes extended media in which the homogeneous state is oscillatory and in the vicinity of a Hopf bifurcation [21] (though its qualitative behavior often seems to reproduce behavior of real systems that are not near a Hopf bifurcation). For a homogeneous system the parameters α and β are real constants. Furthermore, the imaginary part of $\mu=\gamma+i\Omega$ can be eliminated by the replacement, $A\rightarrow A\exp(i\Omega t)$, while γ can be scaled to unity by the replacements $\mathbf{x}\rightarrow\mathbf{x}/\sqrt{\gamma}$, $t\rightarrow t/\gamma$, $A\rightarrow\sqrt{\gamma}A$. Thus in the case of a homogeneous medium it suffices to consider $\mu=1$ in Eq. (1). A steadily rotating spiral wave solution to Eq. (1) with $\mu=1$ has the general form [22]

$$A(r,\theta,t)=F(r)\exp\{i[\sigma\theta-\omega_o t+\psi(r)]\}. \tag{2}$$

The topological charge $\sigma=\pm1$ results in a $2\pi\sigma$ phase change of A for a counterclockwise path around the vortex center $(r=0)$. In order that A be continuous and finite at such a phase singularity at $r=0$, we must have that $A(r=0,\theta,t)=0$. The real functions $F(r)\equiv|A|$ and $\psi(r)$ have the asymptotic behavior as r tends to zero of $F\sim r$ and $d\psi/dr\sim r$. For large r, the spiral wave asymptotes to a plane wave of wave number k_o. Substituting a nonlinear constant amplitude plane wave solution, $A\sim\exp(ik_o r-i\omega_o t)$, into Eq. (1) yields the dispersion relation $\omega_o=\alpha+(\beta-\alpha)k_o^2$ and the boundary condition for $F(r)$ for large r. Thus, as r goes to infinity, $d\psi/dr\rightarrow k_o$ and $F\rightarrow\sqrt{1-k_o^2}$.

In an appreciable range of (α,β) parameter space, called the quasifrozen parameter regime, spiral waves are found to be stable solutions and naturally form from perturbations of $A=0$ [23]. In this regime A evolves toward a quasifrozen state in which many spiral waves form, each with its own domain, where A is approximately described by Eq. (2). A spiral's domain is simply the region of space that its waves

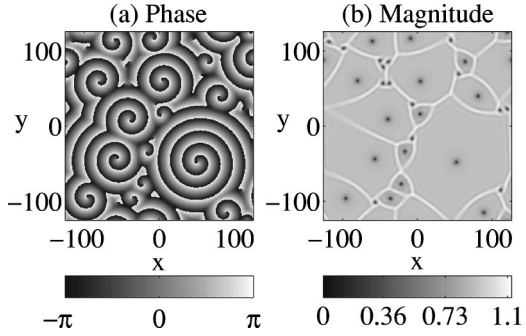

FIG. 1. The phase (a) and magnitude (b) of A at time $t=13\,000$ for the homogeneous case with $\alpha=0.34$ and $\beta=-1.45$ starting from random initial conditions in the unit circle in the complex plane. The system has evolved to a quasifrozen state where the vortices [black spots in (b)] and domain walls [white ridges in (b)] evolve very slowly.

occupy. Spiral domains are separated by narrow domain walls, and after a transient the positions of the domain walls and spiral vortices evolve very slowly [24]. Figures 1(a) and 1(b) show the phase and magnitude of A, respectively, for the homogeneous case ($\mu=1$) after evolving from random initial conditions (A at each grid point is randomly chosen in the unit circle in the complex plane). In Fig. 1 many spirals have formed, each with its own domain. In Fig. 1(a) the spiral vortices are the center of the spiral waves. For Fig. 1(b), spiral vortices can be seen as the dark spots, corresponding to $|A|=0$, and the domain walls are the ridges of lighter shade, corresponding to larger $|A|$. Each spiral has formed with the same frequency ω_o. Away from the vortices and walls $|A|$ is approximately constant, $|A|\simeq\sqrt{1-k_o^2}$.

In other (α,β) parameter regimes, turbulent solutions are possible [23,25]. Turbulent solutions are characterized by the continual creation and annihilation of spiral vortices. As a result, no spiral waves fully develop. The core acceleration regime is found for systems with large values of $|\beta|$ and is characterized by an instability of a spiral wave solution to acceleration of the vortex core leading to disordered (turbulent) solutions. For large values of α the system is in a turbulent regime whose onset is caused by absolute instability of the large r plane waves emanating from the spirals.

We now inquire about the effects of an inhomogeneity that occurs over a large length scale. The expansion yielding the CGLE for a homogeneous medium presumes a situation where the growth rate of the instability is small (i.e., just past a Hopf bifurcation), and this small growth is balanced in the equation by weak (hence lowest order) nonlinearity given by the $|A|^2A$ term and by weak spatial coupling given by the ∇^2A term. A small amount of inhomogeneity causes the small parameter measuring the deviation from the Hopf bifurcation to vary significantly in space. Hence the lowest order effect of the inhomogeneity on Eq. (1) is that the local frequency and growth rate of excitation depend on space. Thus, we set

$$\mu(\mathbf{x})=\gamma(\mathbf{x})+i\Omega(\mathbf{x}), \tag{3}$$

where $\gamma(\mathbf{x})$ and $\Omega(\mathbf{x})$ are slowly varying real functions representing the growth rate and frequency shift, respectively. To lowest order α and β are constant.

The remaining sections of the paper discuss the effects of the inhomogeneity of Eq. (3) in the quasifrozen parameter regime. Section II describes the case in which $\gamma(\mathbf{x})>0$ everywhere, and we discuss the formation of a dominant spiral domain and provide results for the drift velocity of spiral vortices due to the inhomogeneity. In Sec. III we provide qualitative results for the case in which the sign of $\gamma(\mathbf{x})$ is different in different regions of space.

II. QUASIFROZEN REGIME; $\gamma>0$

We begin our investigation of an inhomogeneity by studying the CGLE in the quasifrozen parameter regime with $\gamma(\mathbf{x})>0$ everywhere. We observe that a slow, spatial variation of $\mu(\mathbf{x})$ has two profound effects on the system. The first and perhaps the more striking effect of the inhomogeneity is the formation of a dominant spiral domain. A dominant spiral domain is a domain that increases its size (at the expense of other domains) until it fills the entire system. We show that this is due to an inhomogeneity-induced frequency difference between spirals which results in motion of the domain walls. The second effect of the inhomogeneity is the drift of the spiral centers. The velocity of the drift is linearly related to the gradients of $\mu(\mathbf{x})$ and occurs on a longer time scale than the domain wall motion and the formation of the dominant spiral domain.

We choose the parameter set from the quasifrozen regime of $\alpha=0.34$, $\beta=-1.45$ and study the effect of an inhomogeneity of the following form [26]:

$$\gamma(\mathbf{x})=1+c_1\sin\left(\frac{y}{40}\right)\sin\left(\frac{x}{40}\right),$$
$$\Omega(\mathbf{x})=c_2\sin\left(\frac{y}{40}\right)\cos^2\left(\frac{x}{80}\right)+\omega_o[\,\gamma(\mathbf{x})-1\,] \tag{4}$$

with $c_1=0.3$ and $c_2=0.05$. This choice of (α,β) gives a spiral wave frequency $\omega_o=0.081\,45$ for the homogeneous system. We choose this form of the inhomogeneity in order to satisfy three conditions. The first is periodicity, so that periodic boundary conditions can be used in the numerical solution of Eq. (1). The second condition is that the inhomogeneity should correspond to sufficiently slow, spatial variation in order that perturbation theory can be applied. The third condition is that the maxima and minima of $\gamma(\mathbf{x})$ and $\Omega(\mathbf{x})$ do not coincide. This provides a more general form for the inhomogeneity.

A. Dominant spiral formation

We begin this section by showing the formation of the dominant spiral for the inhomogeneity of Eq. (4). The system is solved on the domain $[-40\pi,40\pi]\times[-40\pi,40\pi]$, which is one wavelength of the inhomogeneity and $\gamma(\mathbf{x})=1$ and $\Omega(\mathbf{x})=0$ on the boundary. As with Fig. 1, the initial condition for each (x,y) is randomly chosen from points in the unit circle of the complex plane. The inhomogeneity is present from the beginning. Figure 2 shows the time evolution of $|A(\mathbf{x},t)|$ normalized by $\sqrt{\gamma(\mathbf{x})}$ and illustrates the formation of a dominant spiral (labeled D in Fig. 2). The normalization $|A(\mathbf{x},t)|/\sqrt{\gamma(\mathbf{x})}$ is an extension of the

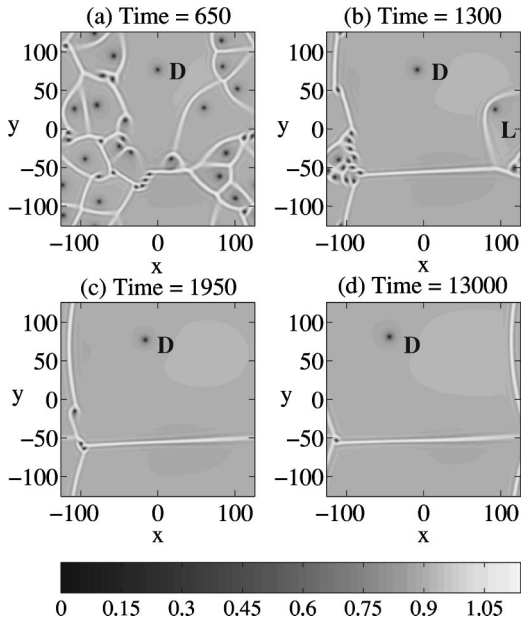

FIG. 2. Time evolution of $|A(\mathbf{x},t)|/\sqrt{\gamma(\mathbf{x})}$ for the inhomogeneity given by Eq. (4). The system is started from random initial conditions chosen in the unit circle of the complex plane. The inhomogeneity is present from the beginning. These time snaps show both the dominant spiral domain formation (labeled *D*) at the expense of the lesser spiral domains (one of which is labeled *L*) and the subsequent drift of vortex *D*.

homogeneous case ($\gamma=$const) in which $|A(\mathbf{x},t)|/\sqrt{\gamma}$ from the spiral wave solution far from the vortex is a constant (depending on α and β), independent of γ.

As in the homogeneous case, the inhomogeneous case initially forms many spiral vortices [see Fig. 2(a)]. The inhomogeneity $\gamma(\mathbf{x})$ does influence the initial distribution of spiral domains since some regions have a faster growth rate than others, but the system still initially generates many spiral domains. The fact that many domains can form is a result of all spirals having exponential growth. For example, consider the spirals labeled *D* and *L* in Fig. 2. For the dominant spiral *D* to grow and dominate the system before the lesser spiral *L* can grow would require that spiral *D* grows and propagates its waves to the location of spiral *L* before spiral *L* has the time to grow. This, however, does not occur since the waves of *D* propagate to *L* in a time greater than that necessary to establish *L* (this might not be the case if we had one region of space with a much larger initial amplitude than the rest of space).

Whereas the homogeneous case creates spirals all with the same frequency $\omega_o=\omega_o(\alpha,\beta)$, the inhomogeneity causes frequency differences between spirals at different locations. Assuming that $\gamma(\mathbf{x})$ and $\Omega(\mathbf{x})$ vary slowly in space, substituting the transformation

$$A(\mathbf{x},t)=\sqrt{\gamma(\mathbf{x})}\hat{A}(\hat{\mathbf{x}})\exp\left(-i[\omega_o\gamma(\mathbf{x})-\Omega(\mathbf{x})]\frac{\hat{t}}{\gamma(\mathbf{x})}\right), \tag{5}$$

where $\hat{\mathbf{x}}=\sqrt{\gamma(\mathbf{x})}\mathbf{x}$ and $\hat{t}=\gamma(\mathbf{x})t$ into Eq. (1), and neglecting terms involving $\nabla\gamma(\mathbf{x})$, we conclude that local spirals exists and are given by the homogeneous equation with the solution $\overline{A}(\hat{\mathbf{x}},\hat{t})=\hat{A}(\hat{\mathbf{x}})\exp(-i\omega_o\hat{t})$. Thus it is expected that the frequency associated with a spiral vortex at $\mathbf{x}$ is well approximated by

$$\omega(\mathbf{x})=\omega_o\gamma(\mathbf{x})-\Omega(\mathbf{x}) \tag{6}$$

when the inhomogeneity length scale is much greater than the vortex diameter. As shown below, this frequency difference between spirals at different locations, Eq. (6), results in the motion of the domain walls observed in Fig. 2. We note that an inhomogeneity is only one of several ways in which spirals can develop with different frequencies. Aranson *et al.*, considering the homogeneous CGLE, investigate the stability of a symmetric two-spiral state against asymmetric perturbations [27]. They find that the situation is unstable in that a slight perturbation from symmetry causes a small frequency difference between the spirals, leading one of them to eventually dominate. Nam *et al.* introduce a chiral symmetry breaking term, which results in spirals with frequencies dependent on their topological charge [28].

To investigate the motion of the domain walls, we consider the vortices to be approximately stationary in space. As shown in the next subsection, there is an inhomogeneity-induced vortex velocity which is of order $|\nabla\gamma/\gamma|$. When the domain size is much larger than $|\nabla\gamma/\gamma|^{-1}$, the domain wall velocity will turn out to be much faster than the vortex velocity, and our assumption of stationary vortices is a good approximation. We begin with the condition that the phase of *A* must match across a domain wall [24,28]. For a homogeneous system, the phase of the interior of any particular domain is described by an Archimedean spiral [24], $\phi_i=\sigma_i\theta_i+k_ir_i-\omega_it+C_i$, where θ_i and r_i are the polar coordinates measured from the center of the ith spiral; σ_i, k_i, ω_i, and C_i are the topological charge, radial wave number, angular frequency, and phase constant, respectively, of the ith spiral. For a slowly varying inhomogeneity, the phase of *A* can be found by a WKB approach since the wavelength of the inhomogeneity is much greater than the wavelength of the spiral wave. Locally, we can assume plane wave solutions of the form $e^{i[\mathbf{k}(\mathbf{x})\cdot\mathbf{x}-\omega t]}$ and, plugging into Eq. (1), obtain a local dispersion relation

$$\omega=\alpha\gamma(\mathbf{x})-\Omega(\mathbf{x})+(\beta-\alpha)k^2. \tag{7}$$

This local dispersion relation leads to the ray equations

$$\frac{d\mathbf{x}}{dt}=\nabla_{\mathbf{k}}\omega=2(\beta-\alpha)\mathbf{k}, \tag{8}$$

$$\frac{d\mathbf{k}}{dt}=-\nabla\omega=\nabla[\Omega(\mathbf{x})-\alpha\gamma(\mathbf{x})]. \tag{9}$$

Since the phase of *A* is not defined at the vortex, the initial conditions for Eqs. (8) and (9) must be taken at a distance R_o from the vortex center $\mathbf{x}_v$. The initial condition for $\mathbf{x}(t=0)$ is then $\mathbf{x}_v+\mathbf{R}_o$. To find the initial condition for $\mathbf{k}(t=0)$, we set the local dispersion relation, Eq. (7), evaluated at $\mathbf{x}_v+\mathbf{R}_o$ equal to the asymptotic frequency for a vortex located at $\mathbf{x}_v$, Eq. (6),

$$\alpha\gamma(\mathbf{x}_v+\mathbf{R}_o)-\Omega(\mathbf{x}_v+\mathbf{R}_o)+(\beta-\alpha)k^2=\omega_o\gamma(\mathbf{x}_v)-\Omega(\mathbf{x}_v). \tag{10}$$

This is valid as long as R_o is much greater than the core size of the vortex. We also know that $\mathbf{k}(t=0)=k_r(t=0)\hat{\mathbf{r}}+(\sigma/R_o)\hat{\theta}$. This result, combined with Eq. (10), gives the initial condition for $k_r(t=0)$ as

$$k_r(t=0)=\pm\sqrt{\frac{\omega_o\gamma(\mathbf{x}_v)-\Omega(\mathbf{x}_v)+\Omega(\mathbf{x}_v+\mathbf{R}_o)-\alpha\gamma(\mathbf{x}_v+\mathbf{R}_o)}{\beta-\alpha}-\left(\frac{\sigma}{R_o}\right)^2}, \tag{11}$$

where the sign of k_r is chosen so that the group velocity [Eq. (8)] is radially outward, i.e., the vortex is a source of waves. The phase of the ith spiral is given by

$$\phi_i=\int_{\Gamma_i}\mathbf{k}_i(\mathbf{r}_i)\cdot d\mathbf{r}_i-\omega_i t+C_i, \tag{12}$$

where the path Γ_i over which the integration is performed is determined by the solution of the ray equations, Eqs. (8) and (9), with the initial conditions of $\mathbf{x}(t=0)=\mathbf{x}_v+\mathbf{R}_o$ and $\mathbf{k}(t=0)=k_r(t=0)\hat{\mathbf{r}}+(\sigma/R_o)\hat{\theta}$, where $k_r(t=0)$ is given by Eq. (11).

For two spirals (labeled $i=1$ and $i=2$) that share a domain wall, the phase matching condition gives at the position $\mathbf{r}$ on the domain wall,

$$S_1(\mathbf{r})-\omega_1 t+C_1=S_2(\mathbf{r})-\omega_2 t+C_2,$$

where $S_i(\mathbf{r})=\int_{\Gamma_i}\mathbf{k}_i(\mathbf{r}_i)\cdot d\mathbf{r}_i$. We define the equiphase line function $f(\mathbf{r})=S_1(\mathbf{r})-S_2(\mathbf{r})$ [28]. The normal velocity of the domain wall is then [29]

$$\mathbf{v}=\frac{\omega_1-\omega_2}{|\nabla f|}\frac{\nabla f}{|\nabla f|}, \tag{13}$$

whose magnitude can be written as

$$v=\frac{\omega_1-\omega_2}{k_{1,\perp}+k_{2,\perp}}, \tag{14}$$

where $k_{1,\perp}$ and $k_{2,\perp}$ are the wave-number vector components normal to the domain wall evaluated at the domain wall, and the reference positive direction points from region 1 to region 2. The wave-number components $k_{1,\perp}$ and $k_{2,\perp}$ can have either a positive or negative sign depending on the direction of $\mathbf{k}_{1,2}$ that is chosen to satisfy an outward group velocity, Eq. (8). For our system $\beta<\alpha$, making the wave-number components $k_{1,\perp}, k_{2,\perp}<0$. From Eq. (14), we see that if $\omega_2<\omega_1$ then $v<0$ and the domain wall will move away from spiral vortex 2 and toward vortex 1. If $\omega_1<\omega_2$ then $v>0$ and the domain wall will move away from spiral vortex 1. Thus the domain walls of the spiral vortex with the lowest frequency move outward. (For $\beta>\alpha$ the situation is reversed.)

Hence, as time proceeds, the domain of the spiral vortex with the lowest frequency gets bigger, and one expects that eventually this domain will become dominant [30]. For the particular system of Eq. (4) the frequency of a spiral located at $\mathbf{x}$ is

$$\omega(\mathbf{x})=\omega_o-c_2\sin\left(\frac{y}{40}\right)\cos^2\left(\frac{x}{80}\right). \tag{15}$$

The lowest frequency spiral, and thus the predicted dominant spiral, will be the spiral that is closest to the minimum of Eq. (15), $(0,20\pi)$. Indeed, looking at Fig. 2(b), we see that the dominant spiral (labeled D in Fig. 2) is the spiral closest to the point $(0,20\pi)$. Once the domain wall has been pushed close to the lesser spiral [labeled L in Fig. 2(b)], there is a strong interaction between the lesser spiral vortex and the domain wall [15]. We then observe that the domain wall sweeps away spiral L's vortex at the speed of the domain wall, which now becomes

$$v=\frac{\omega_L-\omega_D}{k_{D,\perp}}, \tag{16}$$

where the L and D subscripts denote quantities characterizing lesser and dominant spirals. Equation (16) results from a similar argument to the derivation of Eq. (14) except that now we take the L vortex to move with the same speed as the domain wall. We observe a shift in ω_L as a result of the interaction with the wall. As time proceeds further, L is swept into a domain wall and occupies a negligible domain area. Furthermore, vortices of opposite charge embedded in the domain walls merge and annihilate one another [Figs. 2(b) and 2(c)]. Thus, after some time all the lesser spirals get swept away and the dominant spiral domain occupies nearly all the area [Fig. 2(c)].

The difference in frequency of spirals, Eq. (6), results in the motion of the domain walls that leads to the formation of a dominant spiral domain. Two different regimes of motion, similar to those described in Ref. [15] for excitable media, are observed. Initially, when both spiral vortices are far from the domain wall, each spiral vortex is unaffected by the other and the domain wall moves with a velocity given by Eq. (13). Once the domain wall comes close enough, within one wavelength, to the lesser spiral, there is a very strong interaction between the domain wall and the lesser spiral vortex, causing the lesser spiral to be swept away at the speed of the domain wall.

B. Drift of spiral vortices

Another motion of the spiral vortices, independent from the short-ranged interaction with a domain wall, also occurs. This motion is the drift of spiral vortices due to the inhomogeneity. For the case of a long inhomogeneity length scale, the drift of vortices due to the inhomogeneity is slow compared to the domain wall motion and the motion of the lesser spiral vortices due to domain wall interactions discussed in the previous subsection. In that subsection the slow drift of vortices due to the inhomogeneity was neglected. The slow inhomogeneity-induced spiral motion can be seen by comparing Fig. 2(b) to Fig. 2(d) and observing the dominant

spiral's drift to the left. In the case of an inhomogeneity with a scale length much greater than 1, the drift velocity will be linearly related to the gradient of $\mu(\mathbf{x})=\gamma(\mathbf{x})+i\Omega(\mathbf{x})$. Since, in experiments, the frequency $\omega(\mathbf{x})$ of a spiral is more accessible to measurement than the frequency shift $\Omega(\mathbf{x})$, we recast the inhomogeneity into an inhomogeneity of the growth rate $\gamma(\mathbf{x})$ of homogeneous perturbations from $A=0$ and an inhomogeneity of the frequency $\omega(\mathbf{x})$, Eq. (6);

$$\mu(\mathbf{x})=\gamma(\mathbf{x})(1+i\omega_o)-i\omega(\mathbf{x}).$$

(Another strong reason for preferring use of $\nabla\omega$, rather than $\nabla\Omega$, in our formulation is that it simplifies the analysis [e.g., see Eq. (24)].) The drift velocity of a spiral vortex depends only on the local properties [i.e., $\nabla\gamma(\mathbf{x})$ and $\nabla\omega(\mathbf{x})$] of the inhomogeneity [10]. A general form of the drift velocity of a spiral vortex located at $\mathbf{x}_o$ which is linear in the gradients of the inhomogeneity is

$$\mathbf{v}(\mathbf{x}_o)=-m_{\gamma\|}\frac{\nabla\gamma(\mathbf{x}_o)}{\gamma(\mathbf{x}_o)}+\sigma m_{\gamma\perp}\hat{\mathbf{z}}\times\frac{\nabla\gamma(\mathbf{x}_o)}{\gamma(\mathbf{x}_o)} -m_{\omega\|}\frac{\nabla\omega(\mathbf{x}_o)}{\gamma(\mathbf{x}_o)}+\sigma m_{\omega\perp}\hat{\mathbf{z}}\times\frac{\nabla\omega(\mathbf{x}_o)}{\gamma(\mathbf{x}_o)}, \tag{17}$$

where σ is the topological charge of the vortex. As will become evident from the subsequent analysis, by writing $\mathbf{v}$ in this form [in particular, by our division of the right side by $\gamma(\mathbf{x}_o)$ in Eq. (17)], the m coefficients are independent of σ and of the functions $\gamma(\mathbf{x})$ and $\omega(\mathbf{x})$, and they depend only on α and β.

1. Determining the m's due to gradient of growth rate

We now solve for the velocity coefficients corresponding to the gradient of the growth rate $\gamma(\mathbf{x})$, i.e., $m_{\gamma\|}$ and $m_{\gamma\perp}$. Therefore for this section $\nabla\omega(\mathbf{x})=0$ for all $\mathbf{x}$. We assume that a transformation exists between the inhomogeneous spiral wave solution and the homogeneous solution. We show that this transformation occurs only for a specific value of the velocity of the spiral vortex.

We begin by using the assumption of a slow spatial variation of the inhomogeneity $\mu(\mathbf{x})$ and Taylor expand about the spiral vortex location $\mathbf{x}_o$,

$$\mu(\mathbf{x})\simeq[\gamma(\mathbf{x}_o)+\mathbf{x}_1\cdot\nabla\gamma(\mathbf{x}_o)][1+i\omega_o]-i\omega(\mathbf{x}_o),$$

where $\mathbf{x}_1=\mathbf{x}-\mathbf{x}_o$. For simplicity, we set $\gamma(\mathbf{x}_o)=1$ [31], giving the inhomogeneity

$$\mu(\mathbf{x})\simeq[1+\mathbf{x}_1\cdot\nabla\gamma(\mathbf{x}_o)][1+i\omega_o]-i\omega(\mathbf{x}_o). \tag{18}$$

We substitute Eq. (18) into the original equation (1) and apply a similar transformation as in Eq. (5),

$$A(\mathbf{x}_1,t)=\sqrt{\Gamma(\mathbf{x}_2)}A_2(\mathbf{x}_2)\exp[-i\omega(\mathbf{x}_o)t_2], \tag{19}$$

$$\mathbf{x}_2=\mathbf{x}_1-\mathbf{v}t,$$

$$t_2=t,$$

where $\Gamma(\mathbf{x}_2)=1+\mathbf{x}_2\cdot\mathbf{e}_\gamma$ and $\mathbf{e}_\gamma=\nabla\gamma(\mathbf{x}_o)$. This transforms the system into a comoving frame where $\mathbf{v}$ is the velocity of the spiral vortex in the original system. By assuming that $|\mathbf{e}_\gamma|$ and $|\mathbf{v}|$ are of $O(\epsilon)$ and neglecting terms of $O(\epsilon^2)$, Eq. (1) becomes

$$-i\omega_o A_2-\mathbf{v}\cdot\nabla_2 A_2=A_2-(1+i\alpha)|A_2|^2A_2 +\Gamma^{-3/2}(\mathbf{x}_2)(1+i\beta)\nabla_2^2[\sqrt{\Gamma(\mathbf{x}_2)}A_2], \tag{20}$$

where the expansions for $\Gamma(\mathbf{x}_2)$ out to $O(\epsilon)$ were used. We see that Eq. (20) is almost in the form of the homogeneous system except for the $\mathbf{v}\cdot\nabla_2 A_2$ and $\Gamma^{-3/2}(\mathbf{x}_2)(1+i\beta)\nabla_2^2[\sqrt{\Gamma(\mathbf{x}_2)}A_2]$ terms. In order to reduce $\Gamma^{-3/2}(1+i\beta)\nabla_2^2[\sqrt{\Gamma}A_2]$ to a term of the form $(1+i\beta)\nabla_2^2A_2$ as in the original CGLE, we make the following nonlinear coordinate transformation:

$$x_3=x_2+(x_2^2-y_2^2)e_{\gamma x}/4+x_2y_2e_{\gamma y}/2,$$

$$y_3=y_2+(y_2^2-x_2^2)e_{\gamma y}/4+x_2y_2e_{\gamma x}/2,$$

$$t_3=t_2,$$

$$A_2(\mathbf{x}_2)=A_3(\mathbf{x}_3)\exp[i\mathbf{k}_\epsilon\cdot\mathbf{x}_3],$$

where $|\mathbf{k}_\epsilon|$ is of order $O(\epsilon)$. This coordinate transformation gives

$$-i\omega_o A_3-\mathbf{v}\cdot\nabla_3 A_3=A_3-(1+i\alpha)|A_3|^2A_3 +(1+i\beta)[\nabla_3^2A_3+(2i\mathbf{k}_\epsilon+\mathbf{e}_\gamma)\cdot\nabla_3A_3].$$

This equation reduces to the same form as the homogeneous system if the ∇_3A_3 terms cancel. Thus the drift velocity $\mathbf{v}$ is

$$-\mathbf{v}=(1+i\beta)[2i\mathbf{k}_\epsilon+\mathbf{e}_\gamma],$$

which upon solving gives

$$\mathbf{k}_\epsilon=-\beta\mathbf{e}_\gamma/2,$$

$$\mathbf{v}=-(1+\beta^2)\mathbf{e}_\gamma. \tag{21}$$

Transforming back to the original coordinate frame and allowing $\gamma(\mathbf{x}_o)$ to be any positive value gives the velocity of a spiral vortex at $\mathbf{x}_o$ as

$$\mathbf{v}(\mathbf{x}_o)=-(1+\beta^2)\frac{\nabla\gamma(\mathbf{x}_o)}{\gamma(\mathbf{x}_o)}. \tag{22}$$

Comparing Eq. (22) to Eq. (17) we see that

$$m_{\gamma\|}=1+\beta^2, \tag{23}$$

$$m_{\gamma\perp}=0. \tag{24}$$

By applying a set of transformations on the inhomogeneous system, we have found the drift velocity of spiral vortices due to an inhomogeneity in the growth rate, Eq. (22). Spiral vortices move parallel to the gradient of the growth rate when there is no gradient in the frequency.

2. Determining the m's due to gradient of frequency

Having solved for the velocity coefficients $m_{\gamma\parallel}$ and $m_{\gamma\perp}$ in the preceding section, we now solve for the coefficients due to the gradient of the frequency, $m_{\omega\parallel}$ and $m_{\omega\perp}$. We use a numerical technique to find these coefficients. We also give a similarity transformation [22] that relates the values of $m_{\omega\parallel}(\alpha,\beta)$ and $m_{\omega\perp}(\alpha,\beta)$ at a given (α,β) to their values on a one-parameter family of (α,β) values. Thus if the m_ω's are known (or computed) along a line in (α,β) space, then the transformation gives the m_ω's for an area in (α,β) space.

The numerical procedure used to calculate the drift velocity coefficients is similar to that outlined in [25]. We derive a set of perturbation equations and integrate them out to large r. We match this solution to the asymptotic solution for large r to obtain a set of matching constants (denoted as $C^{(a)}$ and $C^{(b)}$ below). The requirement that the perturbation remains bounded determines the velocity of the spiral vortices in terms of these matching constants.

We begin by assuming that the solution to the CGLE with the inhomogeneity is a perturbation of the homogeneous CGLE solution (2). Without loss of generality we also set the inhomogeneity to be linear in the x direction only, i.e., $\mu=1+\epsilon x$ where $\epsilon=\epsilon_r+i\epsilon_i$ is complex. Transforming to the comoving frame, we begin with the equation,

$$\partial_t A-\mathbf{v}\cdot\boldsymbol{\nabla}A=(1+\epsilon x)A-(1+i\alpha)|A|^2A+(1+i\beta)\nabla^2A. \tag{25}$$

We insert the ansatz

$$A(r,\theta,t)=[a(r)(1+\Lambda_x r\cos\theta+\Lambda_y r\sin\theta)+u(r,\theta)]\exp\{i[\sigma\theta-\omega_o t+\Phi(r,\theta)]\}$$

into Eq. (25), where $\Phi(r,\theta)=\phi_x(r)\cos\theta+\phi_y(r)\sin\theta$ and $\Lambda_x,\Lambda_y,\phi_x,\phi_y$ are real. For simplicity we also set $\sigma=1$. We assume that

$$\mathbf{v},\Phi,\Lambda_x,\Lambda_y,u$$

all are of order $O(\epsilon)$. Collecting terms of $O(\epsilon^0)$ gives

$$[(1+i\omega_o)-(1+i\alpha)|a|^2+(1+i\beta)\nabla^2]a\exp[i(\theta-\omega_o t)]=0.$$

This is the unperturbed equation with solution $a(r)\exp[i(\theta-\omega_o t)]$. Collecting terms of $O(\epsilon)$ gives

$$\begin{aligned}&-(i\omega_o+1)u+(1+i\alpha)(2|a|^2u+a^2\overline{u})\\&\quad-(1+i\beta)\left(\nabla^2u+\frac{2i}{r^2}\frac{\partial u}{\partial\theta}-\frac{u}{r^2}\right)\\&=\left\{a\epsilon r-2(1+i\alpha)|a|^2a\Lambda r+\left(a'-\frac{a}{r}\right)\nu+(1+i\beta)\right.\\&\quad\times\left[\phi'\left(2ia'+i\frac{a}{r}\right)+ia\phi''-\frac{3ia}{r^2}\phi\right.\\&\quad\left.\left.+\left(2a'-\frac{2a}{r}\right)\Lambda\right]\right\}\frac{\exp(i\theta)}{2}+\left\{a\epsilon r-2(1+i\alpha)\right.\\&\quad\times|a|^2a\overline{\Lambda}r+\left(a'+\frac{a}{r}\right)\overline{\nu}+(1+i\beta)\\&\quad\times\left[\overline{\phi}'\left(2ia'+i\frac{a}{r}\right)+ia\overline{\phi}''+\frac{ia}{r^2}\overline{\phi}\right.\\&\quad\left.\left.+\left(2a'+\frac{2a}{r}\right)\overline{\Lambda}\right]\right\}\frac{\exp(-i\theta)}{2},\end{aligned} \tag{26}$$

where $\Lambda=\Lambda_x-i\Lambda_y$, $\phi(r)=\phi_x(r)-i\phi_y(r)$, and $\nu=v_x-iv_y$. The prime denotes differentiation with respect to the argument and the bar denotes the complex conjugate. Since the only angular dependence in Eq. (26) is $\exp(i\theta)$ and $\exp(-i\theta)$, we now let

$$u(r,\theta)=u_o(r)+u_+(r)\exp(i\theta)+u_-(r)\exp(-i\theta).$$

We also substitute $\phi_x(r)=r^2\gamma_x/2$ and $\phi_y=r^2\gamma_y/2$ where γ_x,γ_y are real constants into Eq. (26) and collect terms of the same angular dependence. We express the resulting equations in terms of the following operators [32], whose coefficients depend on r and the zeroth order solution $a(r)$:

$$l_-=-(1+i\beta)\nabla_r^2-(i\omega_o+1)+2(1+i\alpha)|a|^2,$$

$$l_o=l_-+(1+i\beta)/r^2,$$

$$l_+=l_-+4(1+i\beta)/r^2,$$

$$g=(1+i\alpha)a^2.$$

This gives the following equations:

$$l_o u_o+g\overline{u_o}=0, \tag{27}$$

$$\begin{aligned}l_+u_++g\overline{u}_-&=\frac{1}{2}\left\{\nu\left(a'-\frac{a}{r}\right)+(1+i\beta)\left[\frac{ia}{2}\gamma+2\left(a'-\frac{a}{r}\right)\Lambda\right]\right.\\&\quad+[a\epsilon-2(1+i\alpha)|a|^2a\Lambda\\&\quad\left.+(1+i\beta)2ia'\gamma]r\right\},\end{aligned} \tag{28}$$

$$\begin{aligned}\overline{l}_-\overline{u}_-+\overline{g}u_+&=\frac{1}{2}\left\{\nu\left(\overline{a}'+\frac{\overline{a}}{r}\right)+(1-i\beta)\right.\\&\quad\times\left[\frac{-5i\overline{a}}{2}\gamma+2\left(\overline{a}'+\frac{\overline{a}}{r}\right)\Lambda\right]\\&\quad+[\overline{a\epsilon}-2(1-i\alpha)|\overline{a}|^2\overline{a}\Lambda\\&\quad\left.-(1-i\beta)2i\overline{a}'\gamma]r\right\},\end{aligned} \tag{29}$$

where we have taken the conjugate of the $\exp(-i\theta)$ component to obtain Eq. (29). For large r, $a(r)\to\sqrt{1-k_o^2}e^{ik_o r}$. In order that the source terms in Eqs. (28) and (29) that vary like r should vanish for large r, we let $\Lambda_y=\gamma_y=0$ and

$$\Lambda=\Lambda_x=\frac{\beta\epsilon_r-\epsilon_i}{2(\beta-\alpha)(1-k_o^2)},$$

$$\gamma=\gamma_x=\frac{\epsilon_i-\alpha\epsilon_r}{2(\beta-\alpha)k_o}.$$

We now look at the behavior of Eqs. (28) and (29) near the origin in order to determine the initial conditions needed to integrate them. The radial dependence of the unperturbed solution $a(r)=F(r)e^{i\psi(r)}$ near the origin varies like $a(r)\sim r$. Substituting this behavior for $a(r)$ into Eqs. (28) and (29) and keeping only order unity terms gives

$$\nabla_r^2 u_+ - \frac{4}{r^2}u_+ = 0, \tag{30}$$

$$\nabla_r^2 \overline{u}_- = -F'(0)\left(\frac{\nu}{1-i\beta}+2\Lambda\right), \tag{31}$$

where $F'(0)$ is the derivative of $F(r)$ from the homogeneous solution (2) evaluated at $r=0$. The integration of Eqs. (30) and (31) under the conditions that $u_+(0)=0$ and $\overline{u}_-(0)=0$ (the field A must vanish at the vortex) gives the following solutions for small r:

$$u_+(r)\simeq hr^2,$$

$$\overline{u}_-(r)\simeq -r^2F'(0)\left(\frac{\nu}{1-i\beta}+2\Lambda\right),$$

with h an arbitrary constant.

To find the asymptotic solution of the perturbation equations, we look at their behavior for large r, which is described by taking the asymptotic limit of Eqs. (28) and (29), i.e., $\nabla_r^2\to\partial_r^2$, $a(r)\to\sqrt{1-k_o^2}e^{ik_or}$, and the $1/r^2$ in l_+ can be dropped. We let $u_+=q_+\exp[r(\lambda+ik_o)]$ and $\overline{u}_-=\overline{q}_-\exp[r(\lambda-ik_o)]$ and obtain the characteristic equation [32]

$$\lambda\{\lambda^3(1+\beta^2)+2\lambda[2k_o^2(1+\beta^2)-(1+\alpha\beta)(1-k_o^2)] + 4k_o(\beta-\alpha)(1-k_o^2)\}=0. \tag{32}$$

The cubic polynomial inside the curly brackets has either three real roots or one real and two complex conjugate roots. In both situations, two of the roots will have positive real parts and the other root will have a negative real part. We refer to the case for which two of the roots are complex conjugate pairs as the oscillatory range [25] and restrict ourselves to this case. In this regime the asymptotic solution is

$$u_+=C^{(a)}\exp[(\lambda_a+ik_o)r]+C^{(b)}\exp[(\lambda_b+ik_o)r], \tag{33}$$

where $C^{(a)}$ and $C^{(b)}$ are constants and $\lambda_a=\overline{\lambda}_b$ with $\mathrm{Re}(\lambda_a)>0$.

In order that the perturbation remains bounded we require that $C^{(a)}=0=C^{(b)}$. Since Eqs. (28) and (29) are linear in ϵ_r, ϵ_i, and ν, the full asymptotic solution of u_+ (i.e., $C^{(a)}$ and $C^{(b)}$) is given by a linear superposition of solutions for the four cases

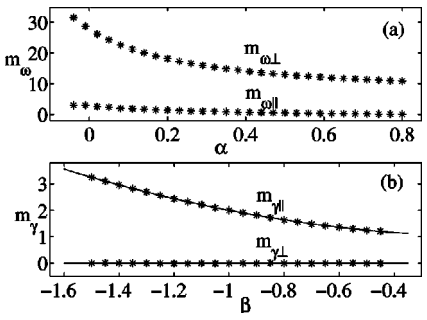

FIG. 3. (a) Velocity coefficients $m_{\omega\perp}$ and $m_{\omega\parallel}$ plotted versus α with $\beta=-1$. (b) Velocity coefficients $m_{\gamma\parallel}$ and $m_{\gamma\perp}$ plotted versus β with $\alpha=0.43$. Shows both the numerically computed values (*) and theoretical predictions (solid line) from Eqs. (23) and (24).

$$\epsilon_r=1,\epsilon_i=0,\nu=0,h=0,$$

$$\epsilon_r=0,\epsilon_i=1,\nu=0,h=0,$$

$$\epsilon_r=0,\epsilon_i=0,\nu=1,h=0,$$

$$\epsilon_r=0,\epsilon_i=0,\nu=0,h=1,$$

where the last case is for the homogeneous equations (right hand side equals zero). For each of these cases, constants $C_j^{(a)}$ and $C_j^{(b)}$ are found by integrating Eqs. (28) and (29) outward from the spiral defect and fitting to the asymptotic solution (33), where $j=r,i,\nu,h$, corresponding to the first, second, third, and fourth of the situations listed above. In order that the perturbation u remains bounded it is necessary that

$$\begin{bmatrix}C^{(a)}\\C^{(b)}\end{bmatrix}=\epsilon_r\begin{bmatrix}C_r^{(a)}\\C_r^{(b)}\end{bmatrix}+\epsilon_i\begin{bmatrix}C_i^{(a)}\\C_i^{(b)}\end{bmatrix}+\nu\begin{bmatrix}C_\nu^{(a)}\\C_\nu^{(b)}\end{bmatrix}+h\begin{bmatrix}C_h^{(a)}\\C_h^{(b)}\end{bmatrix}=0.$$

This gives two equations with two unknowns, ν and h. We can then solve for $\nu=v_x-iv_y$ to find the velocity in terms of the gradients of the inhomogeneity, ϵ_r and ϵ_i, and thus find the m coefficients.

For the specific example shown in Fig. 2 ($\alpha=0.34,\beta=-1.45$), $m_{\omega\parallel}=1.212$ and $m_{\omega\perp}=20.550$. The results for the velocity coefficients $m_{\omega\parallel}$ and $m_{\omega\perp}$ for $\beta=-1$ versus α are shown in Fig. 3(a). This procedure also finds the velocity coefficients $m_{\gamma\parallel}$ and $m_{\gamma\perp}$ and shows good agreement with Eqs. (23) and (24), [see Fig. 3(b)]. Having now found all the velocity coefficients, the velocity of a spiral vortex located at $\mathbf{x}$ is

$$\mathbf{v}(\mathbf{x})=-(1+\beta^2)\frac{\nabla\gamma(\mathbf{x})}{\gamma(\mathbf{x})}-m_{\omega\parallel}\frac{\nabla\omega(\mathbf{x})}{\gamma(\mathbf{x})}+\sigma m_{\omega\perp}\hat{\mathbf{z}}\times\frac{\nabla\omega(\mathbf{x})}{\gamma(\mathbf{x})}. \tag{34}$$

The numerical computation of $m_{\omega\parallel}(\alpha,\beta)$ and $m_{\omega\perp}(\alpha,\beta)$ of Fig. 3(a) gives these coefficients for $\beta=-1$ and $0.8\geqslant\alpha\geqslant-0.05$. It is of interest to consider other (α,β) values. Fortunately, an analytic transformation, previously used [22] for the standard CGLE (without inhomogeneity), can be adapted for this purpose. In particular, given knowledge of $m_{\omega\parallel}$ and $m_{\omega\perp}$ for a particular set of (α,β) parameter values, it is possible to extend this knowledge to knowledge of $m_{\omega\parallel}$ and $m_{\omega\perp}$ at all points on a curve in (α,β) parameter space

[where the curve passes through the original (α,β) values]. Thus the information in Fig. 3(a), which gives $m_{\omega\|}$ and $m_{\omega\perp}$ along a line $(\beta=-1)$ in (α,β) space, can be extended to cover a two-dimensional region of (α,β) space. The transformation accomplishing this is derived in the Appendix, where we find that

$$m_{\omega\|}(\alpha',\beta')=\chi m_{\omega\|}(\alpha,\beta)+\frac{\Delta(1+\beta^2)\chi}{1+\omega_o\Delta}, \tag{35}$$

$$m_{\omega\perp}(\alpha',\beta')=\chi m_{\omega\perp}(\alpha,\beta), \tag{36}$$

$$\Delta=\frac{\alpha-\alpha'}{1+\alpha'\alpha}=\frac{\beta-\beta'}{1+\beta'\beta}, \tag{37}$$

where Δ is a free parameter, $\chi=(1+\omega_o\Delta)^2/(1+\beta\Delta)^2$, and $\omega_o=\omega_o(\alpha,\beta)$ is the homogeneous frequency. As an example, we transform the coefficients for $\alpha=0.34$, $\beta=-1.45$ ($\omega_o=0.081\,45$, $m_{\omega\|}=1.212$, and $m_{\omega\perp}=20.550$) to the point $\alpha'=0.5586,\beta'=-1$ [corresponding to Fig. 3(a)]. We find that $m_{\omega\|}(\alpha',\beta')=0.383$ and $m_{\omega\perp}(\alpha',\beta')=12.434$, which agree well with the measured values from Fig. 3(a) of $m_{\omega\|}=0.393$ and $m_{\omega\perp}=12.425$.

3. Comparison of theory and numerics

Having found the velocity of a vortex in an inhomogeneity, we are now ready to compare our results with numerical simulations of the full equation, Eqs. (1) and (3). For this purpose, it is useful to view the equation of motion for a vortex located at $\mathbf{x}$ as a dynamical system, $d\mathbf{x}/dt=\mathbf{v}(\mathbf{x})$, where $\mathbf{v}(\mathbf{x})$ is given by Eq. (34). This system will, in general, have attractors (i.e., long time asymptotic motions). According to the Poincaré-Bendixson theorem, the only finite attractors to be expected for motion in the plane (R^2) either are periodic or else involve fixed points [33]. [Our numerical simulations use doubly periodic boundary conditions and thus topologically correspond to motion on a two-dimensional toroidal surface (T^2).] In the following we compare our theory for the inhomogeneity-induced vortex motion, Eq. (34), to numerical simulations with two different forms of the inhomogeneity. For both cases we use the parameters $\alpha=0.34$ and $\beta=-1.45$, which give $\omega_o=0.081\,45$, $m_{\omega\|}=1.212$, and $m_{\omega\perp}=20.550$. The first form is given by Eq. (4) and has already been extensively discussed. This form yields a fixed point attractor. The second form for the inhomogeneity (introduced below) yields periodic motion (also called a limit cycle attractor). Nishiyama [5] reports both fixed point and limit cycle attractors for spiral vortices in *Dictyostelium* experiments.

Case 1: Fixed point attractor for Eq. (34). The numerical simulation of the fixed point attractor that results from the inhomogeneity given by Eq. (4) is shown in Fig. 2. Here the system has essentially reached a fixed point attractor at time $t=13\,000$ [Fig. 2(d)]. To compare our numerical and theoretical results, we track the vortex location of the dominant spiral from time 650 to time 13 000 and compare that to the integration of Eq. (34) with the initial condition of the spiral vortex location at time 650 from the numerics. These results are summarized in Fig. 4(a); the solid line is for the theory [Eq. (34)] and the open circles are for the numerical data.

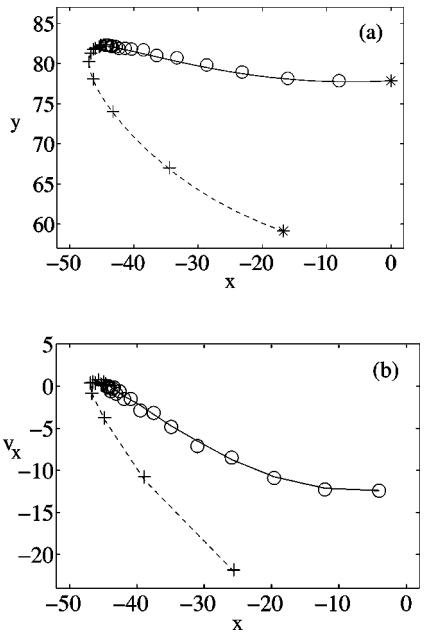

FIG. 4. (a) Vortex trajectory of the dominant spiral to a fixed point. Two different runs are shown. The (*) mark the initial location of the dominant spiral vortex for each run. The lines are from the theory, Eq. (34), and the open circles (○) and crosses (+) are data from numerical simulations. (b) Velocity in the x direction (in units of 10^{-3}) plotted as a function of x.

Figure 4(a) also shows the vortex location for a system started with different initial conditions; the dashed line is for the theory and the crosses are for the numerical data. The velocities in the x direction are shown as functions of x in Fig. 4(b) for both initial conditions and good agreement between theory and numerics can be seen.

Case 2: Limit cycle attractor for Eq. (34). As a simple case where it is easy to understand the possibility that the attractor for vortex motion can be a limit cycle, we let the growth rate be a function of the frequency, $\gamma(\omega)=G(\omega(\mathbf{x}))$. Substituting the growth rate into the velocity (34) gives

$$\mathbf{v}(\mathbf{x})=Q(\omega)\nabla\omega(\mathbf{x})+\sigma m_{\omega\perp}\hat{\mathbf{z}}\times\frac{\nabla\omega(\mathbf{x})}{G(\omega(\mathbf{x}))},$$

where $Q(\omega)=[-(1+\beta^2)G'-m_{\omega\|}]/G(\omega)$ with the prime denoting differentiation with respect to its argument. Thus $d\omega/dt=\mathbf{v}\cdot\nabla\omega=Q(\omega)|\nabla\omega|^2$. This shows that, if $Q(\omega)$ has a zero, $Q(\omega_c)=0$, with $Q'(\omega_c)<0$, then initial conditions near the curve $\omega(\mathbf{x})=\omega_c$ will be attracted to the curve. The curve can then act as a limit cycle attractor. As an example we use our previous inhomogeneity for ω, $\omega(\mathbf{x})=\omega_o-c_2\sin(y/40)\cos^2(x/80)$; and

$$\gamma(\mathbf{x})=K-\chi\omega(\mathbf{x})+\rho[\omega(\mathbf{x})]^2,$$

where K is a constant that is set such that $\gamma>0$ everywhere, $\chi=(m_{\omega\|}+\kappa\omega_c)/(1+\beta^2)$, and $\rho=\kappa/[2(1+\beta^2)]$. For numerical comparison we set $K=1.1$, $\kappa=2000$, $\omega_c=0.03$, and $c_2=0.1$. The results are summarized in Fig. 5, which shows the phase of A at four different times. In this case a single spiral does not dominate the system as in the fixed point

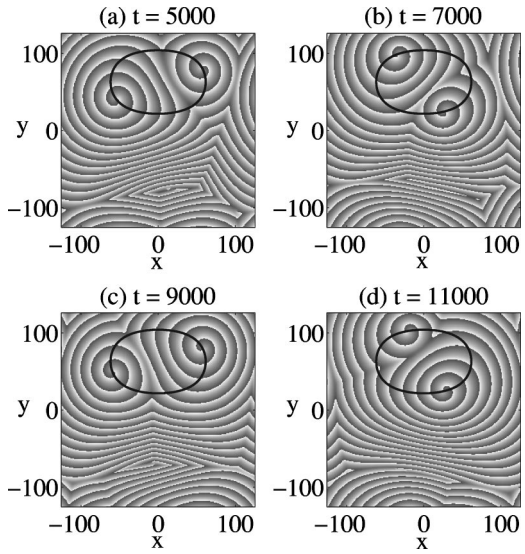

FIG. 5. The phase of A at four different times for the inhomogeneity that produces a limit cycle attractor (solid, black line). The color scale ranges from $-\pi$ to π (gray to white). The two spirals are moving clockwise along the attractor and the period of the limit cycle is approximately 8200 time units. The noticeable wavelength variation results from the relatively large variation in the growth rate (0.8–8.1) chosen for computation convenience. (a) Time = 5000. (b) Time = 7000. (c) Time = 9000. (d) Time = 11 000.

attractor, Fig. 2(d). In Fig. 5, before one spiral can dominate over the other, both spirals are attracted to the limit cycle ($\omega=\omega_c$ contour, solid line in Fig. 5) where both spirals have the same frequency. While the existence of limit cycles does not depend on our choice $\gamma(\mathbf{x})=G(\omega)$, the situation where two defects on the limit cycle always have the same frequency is a special consequence of $\gamma=G(\omega)$.

III. QUASIFROZEN REGIME; $\gamma<0$ SUBREGIONS

Since the growth rate is allowed to vary spatially, the possibility exists that the growth rate will actually become negative in some subregion of the system. This corresponds to having a region where small amplitude waves are exponentially decaying. In fact, such a situation is generically expected for an inhomogeneous system as an instability parameter is increased from a stable situation. In this section we briefly study the qualitative effects of such a negative growth rate region.

To study this phenomenon, we again consider the inhomogeneity given by Eq. (4), but now we lower γ by an overall constant factor of Γ,

$$\gamma(\mathbf{x})=1-\Gamma+c_1\sin\left(\frac{y}{40}\right)\sin\left(\frac{x}{40}\right). \tag{38}$$

$\omega(\mathbf{x})$ is still given by Eq. (15). From Eq. (34) we note that the vortex velocity diverges as γ goes to zero. Thus the perturbation expansion used to obtain Eq. (34) breaks down in the region of small $\gamma>0$. This indicates the possibility of new physical effects. To investigate this, we set $\Gamma=0.9$, $c_1=0.3$, $c_2=0.05$, and $\omega_o=0.081\,45$, so that a relatively large region of space has a negative growth rate. The effects of this inhomogeneity are shown in Fig. 6 where inside the white

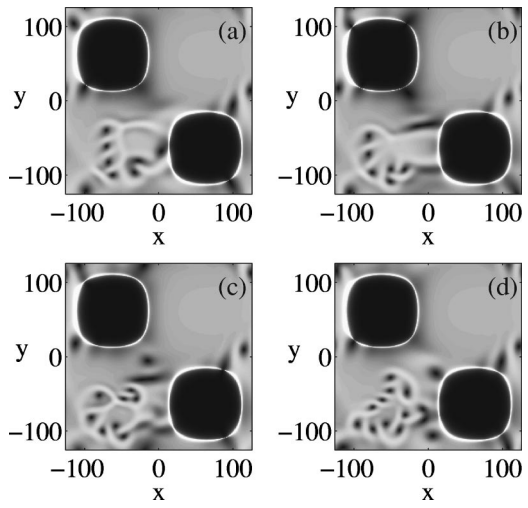

FIG. 6. The normalized magnitude $|A|/\sqrt{|\gamma|}$ at four different times for the inhomogeneity (38). The white circles are the $\gamma=0$ contours and $\gamma<0$ inside them. The color scale is 0–1.2 (black–white). The time sequence shows the ejection of vortices out of the negative growth region. (a) Time = 2875. (b) Time = 2937.5. (c) Time = 3000. (d) Time = 3062.5.

circles the growth rate is negative. Looking at the lower right negative γ region in Figs. 6(b) and 6(c), we see the ejection of vortices out of the negative γ region and into the positive γ region (third quadrant). This results in an increase of vortices [compare Figs. 6(a) and 6(d)]. As time proceeds further, some of these vortices may recombine and annihilate one another. This cycle of ejection and annihilation of vortices leads to a turbulentlike situation where there are no fully developed spiral waves. A similar picture also occurs for a system that has only a small region of space with a negative growth region ($\Gamma=0.71$).

Curiously, only the third quadrant of our system exhibited this turbulentlike phenomenon, whereas the first quadrant remained essentially free of vortices. This phenomenon seems linked with the inhomogeneity of the frequency (38) [ω is larger for $y<0$ (third quadrant) than for $y>0$ (first quadrant)]. When we removed the inhomogeneity of the frequency by setting $c_2=0$, the system no longer exhibited this behavior and the system settled down to having no vortices or spiral waves in either the first or third quadrant.

IV. CONCLUSION

In this paper, we have studied the role of a slowly varying inhomogeneity on the dynamics of spiral waves in the two-dimensional complex Ginzburg-Landau equation. In the quasifrozen parameter regime of the CGLE, the inhomogeneity causes frequency differences between spirals at different locations. As a consequence of this frequency difference, favorably located spirals can grow and dominate the system. The inhomogeneity also results in the motion of the spiral vortices. We have derived an expression for the velocity which is related to the gradients of the inhomogeneity, Eq. (34), and see good agreement with numerical simulations. We also have studied situations in which there are regions of negative growth rate, and observed continual creation and annihilation of vortices when an inhomogeneity in the frequency is present.

ACKNOWLEDGMENTS

M.H. thanks Michael Gabbay and Parvez Guzdar for use of their computer simulation code. This work was supported by the Office of Naval Research.

APPENDIX

In this Appendix we derive the similarity transformation relating $m_{\omega\perp}$ and $m_{\omega\|}$ evaluated at (α,β) to $m_{\omega\perp}$ and $m_{\omega\|}$ evaluated at (α',β'). We introduce a free parameter and then find a set of transformations back to the original system. We can then compare the spiral vortex drift velocity in the original system with that of the system with the free parameter to determine the relation between the drift velocity coefficients in the two systems.

Since we are interested only in the velocity due to the gradient of $\omega(\mathbf{x})$, we start with the inhomogeneity of $\mu(\mathbf{x}) = 1 + i\omega_o - i\omega(\mathbf{x})$ (ω_o is the homogeneous frequency) and Taylor expand about the spiral vortex location $\mathbf{x}_o$,

$$\mu(\mathbf{x}) \simeq 1 + i\omega_o - i\omega(\mathbf{x}_o) - i\mathbf{x}_1 \cdot \boldsymbol{\nabla}\omega(\mathbf{x}_o), \tag{A1}$$

where $\mathbf{x}_1 = \mathbf{x} - \mathbf{x}_o$. We insert this into the CGLE and apply the following transformation:

$$A(\mathbf{x}_1,t) = A_2(\mathbf{x}_2)\exp[-i\omega(\mathbf{x}_o)t_2],$$

$$\mathbf{x}_2 = \mathbf{x}_1 - \mathbf{v}t,$$

$$t_2 = t,$$

which transforms the system to the comoving frame with $\mathbf{v}$ the velocity of the spiral vortex in the original system. We assume that $|\mathbf{e}_\omega| = |\boldsymbol{\nabla}\omega(\mathbf{x}_o)|$ and $|\mathbf{v}|$ are of $O(\epsilon)$. Neglecting terms of $O(\epsilon^2)$, the CGLE becomes

$$-i\omega_o A_2 - \mathbf{v}\cdot\boldsymbol{\nabla}_2 A_2 = (1 - i\mathbf{x}_2\cdot\mathbf{e}_\omega)A_2 - (1+i\alpha)|A_2|^2 A_2 + (1+i\beta)\nabla_2^2 A_2. \tag{A2}$$

We also make the transformation of $A_2(\mathbf{x}_2) \rightarrow A_2(\mathbf{x}_2)\exp[i\mathbf{k}_\epsilon\cdot\mathbf{x}_2]$ where $|\mathbf{k}_\epsilon|$ is of $O(\epsilon)$. This transforms Eq. (A2) into

$$-i\omega_o A_2 - [\mathbf{v} + 2i(1+i\beta)\mathbf{k}_\epsilon]\cdot\boldsymbol{\nabla}_2 A_2 = (1 - i\mathbf{x}_2\cdot\mathbf{e}_\omega)A_2 - (1+i\alpha)|A_2|^2 A_2 + (1+i\beta)\nabla_2^2 A_2.$$

We now introduce the free, real parameter Δ by adding $i\Delta A_2$ to both sides and dividing by $1 + i\Delta A_2$. This leads to the equation

$$-i\left(\frac{\omega_o - \Delta}{1+i\Delta}\right)A_2 - \left(\frac{\mathbf{v} + 2i\mathbf{k}_\epsilon(1+i\beta)}{1+i\Delta}\right)\cdot\boldsymbol{\nabla}_2 A_2 = \left(1 - i\mathbf{x}_2\cdot\frac{\mathbf{e}_\omega}{1+i\Delta}\right)A_2 - \left(\frac{1+i\alpha}{1+i\Delta}\right)|A_2|^2 A_2 + \left(\frac{1+i\beta}{1+i\Delta}\right)\nabla_2^2 A_2. \tag{A3}$$

In order that the imaginary part of the $\boldsymbol{\nabla}_2 A_2$ term vanish we set $2\mathbf{k}_\epsilon = \mathbf{v}\Delta/(1+\beta\Delta)$. We make another set of transformations,

$$\mathbf{x}_3 = \sqrt{\frac{1+\omega_o\Delta}{1+\beta\Delta}}\,\mathbf{x}_2,$$

$$A_3(\mathbf{x}_3) = \sqrt{\frac{1+\alpha\Delta}{1+\omega_o\Delta}}\,A_2(\mathbf{x}_2),$$

and define the following quantities:

$$\omega_o' = \frac{\omega_o - \Delta}{1+\omega_o\Delta},$$

$$\mathbf{v}' = \frac{1+\Delta^2}{\sqrt{1+\omega_o\Delta}(1+\beta\Delta)^{3/2}}\mathbf{v},$$

$$\mathbf{e}_\omega' = \frac{\sqrt{1+\beta\Delta}}{(1+\omega_o\Delta)^{3/2}}\mathbf{e}_\omega,$$

$$\mathbf{e}_\gamma' = -\Delta\mathbf{e}_\omega',$$

$$\beta' = \frac{\beta - \Delta}{1+\beta\Delta},$$

$$\alpha' = \frac{\alpha - \Delta}{1+\alpha\Delta}.$$

Using the transformation and the definitions given above, Eq. (A3) becomes

$$-i\omega_o' A_3 - \mathbf{v}'\cdot\boldsymbol{\nabla}_3 A_3 = [1 + (\mathbf{e}_\gamma' - i\mathbf{e}_\omega')\cdot\mathbf{x}_3]A_3 - (1+i\alpha')|A_3|^2 A_3 + (1+i\beta')\nabla_3^2 A_3. \tag{A4}$$

We examine this inhomogeneity more closely. In the previous calculation of the velocity coefficients due to a gradient in the growth rate γ (see Sec. II B 1), we found that an inhomogeneity of the form $\mu = 1 + (1+i\omega_o)\mathbf{e}_\gamma\cdot\mathbf{x}$ results in a vortex motion parallel to the gradient of γ. Using this result we then let

$$\mathbf{e}_\gamma' - i\mathbf{e}_\omega' = \mathbf{e}_\gamma'(1+i\omega_o') - i(\mathbf{e}_\omega' + \omega_o'\mathbf{e}_\gamma'),$$

where we know that the first term of the right hand side gives a velocity $\mathbf{v}' = -(1+\beta'^2)\mathbf{e}_\gamma'$ from Eq. (21). Therefore we set

$$\mathbf{v}'' = \mathbf{v}' + (1+\beta'^2)\mathbf{e}_\gamma'$$

$$\mathbf{e}_\omega'' = (1 - \omega_o'\Delta)\mathbf{e}_\omega',$$

so that Eq. (A4) becomes

$$-i\omega_o' A_3 - \mathbf{v}'' \cdot \boldsymbol{\nabla}_3 A_3 = (1 - i\mathbf{e}_\omega'' \cdot \mathbf{x}_3)A_3 - (1 + i\alpha')|A_3|^2 A_3 + (1 + i\beta')\nabla_3^2 A_3, \tag{A5}$$

which is of the same form as Eq. (A2). The general velocities for Eqs. (A2) and (A5) are

$$\mathbf{v} = -m_{\omega\parallel}(\alpha,\beta)\mathbf{e}_\omega + \sigma m_{\omega\perp}(\alpha,\beta)\hat{\mathbf{z}} \times \mathbf{e}_\omega, \tag{A6}$$

$$\mathbf{v}'' = -m_{\omega\parallel}(\alpha',\beta')\mathbf{e}_\omega'' + \sigma m_{\omega\perp}(\alpha',\beta')\hat{\mathbf{z}} \times \mathbf{e}_\omega'', \tag{A7}$$

respectively. Now applying the definitions for the primed system and substituting Eq. (A6) into Eq. (A7), we find that

$$m_{\omega\parallel}(\alpha',\beta') = \chi m_{\omega\parallel}(\alpha,\beta) + \frac{\Delta(1+\beta^2)\chi}{1+\omega_o\Delta}, \tag{A8}$$

$$m_{\omega\perp}(\alpha',\beta') = \chi m_{\omega\perp}(\alpha,\beta), \tag{A9}$$

$$\Delta = \frac{\alpha - \alpha'}{1 + \alpha'\alpha} = \frac{\beta - \beta'}{1 + \beta'\beta}, \tag{A10}$$

where Δ is the free parameter, $\chi = (1+\omega_o\Delta)^2/(1+\beta\Delta)^2$, and $\omega_o = \omega_o(\alpha,\beta)$ is the homogeneous frequency. Given a value of (α,β), the second equality of Eq. (A10) gives the equation of a hyperbola in (α',β') space that passes through the point (α,β). If we know $m_{\omega\parallel}$ and $m_{\omega\perp}$ at the single point (α,β) in parameter space, then Eqs. (A8)–(A10) tell us the values of the m_ω's at all points on the hyperbola. For example, using knowledge of the m_ω coefficients along the line $\beta = -1$, we can use the transformation of Eqs. (A8)–(A10) to extend this to knowledge of m_ω's at any point in parameter space.

[1] A. T. Winfree, Chaos **8**, 1 (1998), and references therein.

[2] F. X. Witkowski, L. J. Leon, P. A. Penkoske, W. R. Giles, M. L. Spano, W. L. Ditto, and A. T. Winfree, Nature (London) **392**, 78 (1998).

[3] *Chemical Waves and Patterns*, edited by R. Kapral and K. Showalter (Kluwer Academic, Dordrecht, 1993).

[4] A. J. Durston, Dev. Biol. **37**, 225 (1974).

[5] N. Nishiyama, Phys. Rev. E **57**, 4622 (1998).

[6] Y. A. Astrov, I. Müller, E. Ammelt, and H.-G. Purwins, Phys. Rev. Lett. **80**, 5341 (1998).

[7] M. Markus, Z. Nagy-Ungvarai, and B. Hess, Science **257**, 225 (1992).

[8] A. Belmonte and J.-M. Flesselles, Phys. Rev. Lett. **77**, 1174 (1996); V. Petrov, Q. Ouyang, G. Li, and H. L. Swinney, J. Phys. Chem. **100**, 18 992 (1996).

[9] O. Steinbock, P. Kettunen, and K. Showalter, Science **269**, 1857 (1995).

[10] A. M. Pertsov and Ye. A. Yermakova, Biophysics **33**, 364 (1988).

[11] I. V. Biktasheva, Yu. E. Elkin, and V. N. Biktashev, Phys. Rev. E **57**, 2656 (1998).

[12] A. M. Pertsov, J. M. Davidenko, R. Salomonz, W. Baxter, and J. Jalife, Circ. Res. **72**, 631 (1992).

[13] R. R. Aliev and A. B. Rovinsky, J. Phys. Chem. **96**, 732 (1992).

[14] M. Bär, A. K. Bangia, I. G. Kevrekidis, G. Haas, H.-H. Rotermund, and G. Ertl, J. Phys. Chem. **100**, 19 106 (1996).

[15] M. Vinson, Physica D **116**, 313 (1998).

[16] M. Vinson, A. M. Pertsov, and J. Jalife, Physica D **72**, 119 (1993).

[17] L. Gil, K. Emilsson, and G.-L. Oppo, Phys. Rev. A **45**, R567 (1992).

[18] J. A. Sepulchre and A. Babloyantz, Phys. Rev. E **48**, 187 (1993).

[19] I. Aranson, L. Kramer, and A. Weber, in *Spatio-Temporal Patterns in Nonequilibrium Complex Systems: NATO Advanced Research Workshop*, edited by P. E. Cladis and P. Palffy-Muhoray (Addison-Wesley, Reading, MA, 1995), p. 479.

[20] A. P. Munuzuri, V. Perez-Munuzuri, and V. Perez-Villar, Phys. Rev. E **58**, R2689 (1998).

[21] M. C. Cross and P. C. Hohenberg, Rev. Mod. Phys. **65**, 851 (1993); Y. Kuramoto, *Chemical Oscillations, Waves, and Turbulence* (Springer-Verlag, New York, 1984).

[22] P. Hagan, SIAM (Soc. Ind. Appl. Math.) J. Appl. Math. **42**, 762 (1982).

[23] H. Chaté and P. Manneville, Physica A **224**, 348 (1996); G. Huber, P. Alstrøm, and T. Bohr, Phys. Rev. Lett. **69**, 2380 (1992); I. S. Aranson, L. Aranson, L. Kramer, and A. Weber, Phys. Rev. A **46**, R2992 (1992).

[24] T. Bohr, G. Huber, and E. Ott, Physica D **106**, 95 (1997).

[25] I. Aranson, L. Kramer, and A. Weber, Phys. Rev. Lett. **72**, 2316 (1994).

[26] M. Hendrey, E. Ott, and T. M. Antonsen, Jr., Phys. Rev. Lett. **82**, 859 (1999).

[27] I. Aranson, L. Kramer, and A. Weber, Phys. Rev. E **48**, R9 (1993). This homogeneous mechanism becomes exponentially slow as the domains grow in size. Thus it is not responsible for the relatively fast domination of a single spiral in our inhomogeneous computations [e.g., Fig. 1 (homogeneous) at $t = 13\,000$ and Fig. 2(c) (inhomogeneous) at the earlier time $t = 2000$ are for the same values of α and β, and the same initial conditions].

[28] K. Nam, E. Ott, M. Gabbay, and P. Guzdar, Physica D **118**, 69 (1998).

[29] This argument neglects motion of the vortices such as the slow drift due to the inhomogeneity, Eq. (34).

[30] For $\beta > \alpha$ the wave numbers $k_{1,\perp}, k_{2,\perp} > 0$ and the dominant spiral will have the highest frequency.

[31] Otherwise the transformation $\mathbf{x} \to \mathbf{x}/\sqrt{\gamma(\mathbf{x}_o)}$, $t \to t/\gamma(\mathbf{x}_o)$, and $A \to \sqrt{\gamma(\mathbf{x}_o)}A$ could be used to rescale $\gamma(\mathbf{x}_o)$ to unity.

[32] M. Gabbay, E. Ott, and P.N. Guzdar, Physica D **118**, 371 (1998).

[33] Chaotic or quasiperiodic vortex motion could result if the inhomogeneity had a slow periodic time dependency, or if the gradient length were short enough so that our analysis yielding $d\mathbf{x}/dt = \mathbf{v}(\mathbf{x})$ did not apply. In regard to the latter, see Aranson *et al.* [19], who observe quasiperiodic motion in the case of a strong localized gradient.